

Three-Dimensional J-Resolved H-1 Magnetic Resonance Spectroscopic Imaging of Volunteers and Patients With Brain Tumors at 3T

Yan Li,^{1,2*} Albert P. Chen,² Jason C. Crane,² Susan M. Chang,³ Daniel B. Vigneron,^{1,2,4} and Sarah J. Nelson^{1,2,4}

A method that combines two-dimensional (2D) J-resolved spectroscopy with three spatial dimension magnetic resonance spectroscopic imaging (MRSI) is introduced to measure J-coupled metabolites of glutamate (Glu), glutamine (Gln), myo-Inositol (mI), and lactate (Lac) in the brain and to simultaneously obtain T_2 values of choline (Cho), creatine (Cr), and N-acetyl aspartate (NAA). Relatively few points in the t_1 dimension (six echo times) and a flyback echo-planar trajectory were incorporated in the acquisition to speed up the total acquisition time so that it was within a clinically feasible range (23 min). Data obtained using GAMMA software simulations and from phantoms have shown that the $^4\text{CH}_2$ resonances of Glu can be separated from Gln at 2.35 ppm in TE-averaged spectra. Results from phantoms, six normal volunteers, and four patients demonstrated good signal-to-noise ratio (SNR). The J cross-peaks from the methyl group of Lac were visualized in the 2D spectra from the phantom and the glioma patient, and could be quantified from the spectra at $J = \pm 4.17$ Hz. This technique also enables the evaluation of the changes in metabolite T_2 . Compared with the values in normal white matter, the T_2 values of Cho and Cr were statistically significantly increased in regions of glioma. Magn Reson Med 58:886–892, 2007. © 2007 Wiley-Liss, Inc.

Key words: 2D J-resolved spectroscopy; 3D proton magnetic resonance spectroscopic imaging; brain tumors; 3T; glutamate; lactate

Proton magnetic resonance spectroscopy (MRS) has been widely used to allow assessment of glioma metabolism. Spectra acquired with long echo time (~144 ms) provide metabolites, such as Choline containing compounds (Cho), creatine (Cr), N-acetyl aspartate (NAA), lactate (Lac), and lipid (Lip), can help in distinguishing between normal brain and brain tumors, and different brain tumor types. In

vivo brain tumors show an increase of Cho due to increased membrane synthesis in neoplasm and a decrease of the neuronal marker NAA. Lac is a marker of anaerobic metabolism, and its CH_3 component (1.3 ppm) often overlaps with CH_2 groups in long alkyl chains of Lip arising from necrosis or subcutaneous Lip. Spectral editing using J-difference methods have been applied to separate Lac from Lip for the quantification of Lac, which can be used to assess the malignancy of tumors (1,2). However, there is often a loss in signal-to-noise ratio (SNR) during subtraction, and the methods are sensitive to phase and frequency variations between two acquisitions.

At short echo times (<40 ms), glutamate (Glu), glutamine (Gln), and myo-Inositol (mI) also appear in the spectrum, but peak overlap and complex coupling patterns make it difficult to isolate individual components, even at higher field strength. Two-dimensional J-resolved spectroscopy, a technique that has been performed on high-resolution NMR spectrometers for decades, more recently has been applied for in vivo MRS studies on clinical MR scanners (3,4). This technique enables the separation of J-coupling information from chemical shift by encoding J-coupling in the t_1 dimension of a 2D spectrum using different echo times. The addition of the second frequency dimension also allows the separation of Lac from Lip (3). For in vivo studies, the number of echo times used for J-resolved MRS is typically 32 or 64 with F_1 spectral resolution of ~3 Hz based upon the coupling constant of Lac (~7 Hz) (5).

Recent studies have used this acquisition scheme in conjunction with averaging across the different echo times in the t_1 domain to offer unobstructed detection of Glu at 3T, which has been termed TE-averaged point-resolved spectral selection (PRESS) (6). Since data are acquired at multiple echo times, it also enables measurement of T_2 relaxation times of uncoupled resonances, which are important for accurate metabolite quantification (7). In prior studies, this method has been implemented as both a single-voxel acquisition with 8-cm³ spatial resolution (6) and a 2D J-resolved magnetic resonance spectroscopic imaging (MRSI) pulse sequence (8) with one spatial dimension being acquired using phase encoding and the other using a flyback echo-planar trajectory (9) at 3T. The latter was acquired with 1.8 cm³ nominal spatial resolution. The TE-averaged PRESS has provided more accurate quantification of Glu and offers the possibility of simultaneously measuring T_2 but has only been applied to brain tumors in single-voxel acquisition mode (7). The extreme heterogeneity of gliomas means that multivoxel spectroscopic imaging with higher spatial resolution is required to provide

¹University of California, San Francisco/University of California, Berkeley (UCSF/UCB) Joint Graduate Group in Bioengineering, San Francisco, California, USA.

²Surbeck Laboratory of Advanced Imaging, Department of Radiology, University of California, San Francisco, San Francisco, California, USA.

³Department of Neurological Surgery, University of California, San Francisco, San Francisco, California, USA.

⁴Program in Bioengineering, University of California, San Francisco, San Francisco, California, USA.

Grant sponsor: UC Discovery, in conjunction with GE Healthcare; Grant numbers: LSIT01-10107, ITL-BIO04-10148; Grant sponsor: National Institutes of Health (NIH); Grant numbers: R01 CA059880, P50 CA97257.

This work was presented in part at the 15th Annual Meeting of ISMRM, Berlin, Germany, 2007.

*Correspondence to: Yan Li, UCSF Radiology Box 2532, Byers Hall, 1700 4th Street, San Francisco, CA 94143-2532. E-mail: yan.li@radiology.ucsf.edu
Received 8 February 2007; revised 15 August 2007; accepted 19 August 2007.

DOI 10.1002/mrm.21415

Published online in Wiley InterScience (www.interscience.wiley.com).

© 2007 Wiley-Liss, Inc.

more detailed information within the tumoral and peritumoral regions.

The goal of this study was to develop a new acquisition scheme that can provide data within a clinically feasible acquisition time and to develop postprocessing methods for interpretation of 2D J-resolved PRESS MRSI data with three spatial dimensions. This includes the development of strategies for improving the quantification of metabolites from these spectra using prior information concerning the J-coupling of metabolites such as Glu, mI, and Lac, as well as correcting for relaxation times of metabolites whenever possible.

MATERIALS AND METHODS

Simulated Data

PRESS spectra of Glu and Gln with TE values starting at 35 ms in six steps of 40 ms were simulated using GAMMA software (10) using prior knowledge of peak locations and J-coupling constants (5). The spectra were created with 1024 dwell points and a sweep width of 2000 Hz. A 4-Hz Lorentzian apodization in the t_2 dimension, zero filling to 2048 points, and Fourier transform were applied and the resultant data were averaged in the t_1 dimension.

MR Data

All the empirical studies were performed using a transmit body coil and eight-channel phased array coil for signal reception with a 3T GE Signa scanner (GE Healthcare, Waukesha, WI, USA). The MR scans included the acquisition of both anatomic and spectroscopic imaging data.

Anatomical MR images comprised T_1 -weighted sagittal scout images (TR/TE = 70 ms/2 ms at 3T), axial fluid attenuated inversion recovery (FLAIR) (TR/TE/TI = 10,002 ms/127 ms/2200 ms) and T_1 -weighted spoiled gradient echo (SPGR) image (TR/TE = 26 ms/3 ms). In addition, proton density-weighted gradient echo images were acquired using the manufacturer-provided parallel imaging calibration sequence to obtain the estimates of coil sensitivities (TR/TE = 150 ms/2 ms) for the combination of the spectral data from each of the eight channels.

The J-resolved spectra were localized in three spatial dimensions using PRESS volume selection. To show the reliability of the relative position of metabolites, a single-voxel 2D J-resolved acquisition was performed in the metabolite phantoms with 2000 Hz sweep width and 1024 dwell point, resulting in spectral resolution in the F_2 dimension of ~ 1.95 Hz. The increment delay ($t_1/2$) of the J-resolved acquisition was added before and after the final refocusing RF pulse in the PRESS sequence to encode t_1 . The initial echo time was 35 ms. Six increments in the t_1 dimension were acquired over a 25-Hz spectral bandwidth to yield an F_1 resolution of 4.17 Hz per point.

The 3D J-resolved MRSI data were acquired utilizing a flyback echo-planar gradient trajectory (9), which allowed the encoding of one spatial dimension and the spectral dimension during a single readout, to speed up the acquisition time. The flyback echo-planar gradient was designed to provide a spatial resolution of 1 cm and was applied in the right/left direction for an FOV of 16 cm (16 spatial points). The spectral data were collected with 712 dwell

points and 988 Hz sweep width, which provides ~ 1.39 Hz spectral resolution per point in the F_2 dimension. The 3D spectral array size was $16 \times 12 \times 8$ (right-left [RL] \times anterior-posterior [AP] \times superior-inferior [SI]) and the nominal spatial resolution was 1 cm³. With a TR of 1.2 s and a number of excitations (NEX) of 2, the total acquisition time for 3D J-resolved MRSI was 23 min.

Study Population

An in vitro basis set from phantoms containing individual metabolites (50 mM Cho, 50 mM Cr, 50 mM NAA, 100 mM Glu, 100 mM Gln, 200 mM mI, and 200 mM Lac) was prepared by performing single-voxel 2D J-resolved acquisition on each phantom. To test the hypothesis that the 2D spectral cross-peaks of Lac can be separated from the overlapping Lips, the Lac phantom was covered with a thick piece of bacon and data was acquired using single-voxel 2D J-resolved acquisition.

A standard GE MRS phantom (12.5 mM NAA, 10 mM Cr, 3 mM Cho, 12.5 mM Glu, 7.5 mM mI, and 5 mM Lac), six healthy volunteers, and four patients with different kinds of primary brain tumors were included in the study. Patient diagnoses were: one undefined glioma (patient A) and three glioblastoma multiforme (GBM) patients (patients B, C, and D). To test the reproducibility of such data, we scanned the head phantom and two of the volunteers twice while positioning the excited volumes in similar regions.

POSTPROCESSING AND ANALYSIS

Postprocessing was performed on a Linux Cluster in our laboratory (13 Sun Fire V60x Intel Xeon servers [2 \times 2.8 GHz, 1-GB memory], 4 Sun Fire V20z AMD Opteron servers [2 \times 2.4 GHz, 4-GB memory]) running Sun's N1 Grid Engine (Sun Microsystems, Santa Clara, CA, USA). Spectral arrays from the eight-channel coil were processed in parallel on separate central processing units (CPUs) and the signals were combined using in-house developed software that weighted the data by their coil sensitivities (11,12). Relative metabolite ratios were quantified using the LCModel package (13) for voxels within the PRESS box ($8 \times 8 \times 4$) on a single SunBlade 1000 Workstation (Sun Microsystems).

The single voxel data were processed with phase and frequency corrections using the internal water signal, apodized with a 4-Hz Lorentzian function, zero-filled to 2048 points, and fast Fourier transformed (FFTed) in the t_2 dimension. A second FFT was applied in the t_1 dimension and a 45° rotation of the 2D spectra was performed to separate chemical shift and J-coupling information.

The 3D J-resolved MRSI data that were acquired using flyback readout trajectory were reordered to correspond to a rectilinear grid with resampling and phase corrections (9), followed by processing with first-point phasing and apodization in the t_2 domain. The eight-channel data were then combined in the t_2 domain. To estimate relative metabolite levels, the combined data were averaged in the t_1 domain and then quantified using the LCModel package. Spectra were fitted between 4.0 ppm and 1.0 ppm. Metabolite ratios included in the analysis were those with rela-

tive Cramér-Rao lower bounds (CRLB) lower than 5% for Cho, Cr, and NAA, 20% for mI and Glu, and 25% for Glx (Glu+Gln). The peak heights of Cho, Cr, NAA, and Glu were computed automatically using in-house software for each voxel within the excited region from the TE-averaged data (14). The SNR of individual metabolites were estimated by dividing the heights of the peaks by the standard deviation (SD) of the noise from the peak-free region at the right end of the spectrum.

Six different echo-time spectra of the 3D J-resolved MRSI were each processed prior to averaging in the t_1 dimension to estimate the T_2 of each metabolite. The peak heights of Cho at 3.22 ppm, Cr-CH₃ at 3.02 ppm, and NAA at 2.02 ppm were estimated from each echo-time spectra (14), and then fitted to a single exponential function to calculate T_2 metabolic relaxation times using the SAGETM software package (General Electric, Milwaukee, WI, USA). The 2D spectra with three spatial dimensions were generated by applying a second FFT and 45° rotation in the t_1 dimension. Only the T_2 values with variances of the fit residue smaller than 10% were included in the analysis.

The coefficient of variance (CV) for reproducibility was calculated using the formula, $CV = \sqrt{\sum_{i=1}^m SD_i^2 / m} / \bar{X} \times 100\%$, where the SD_i are the standard deviations of normalized peak heights in the voxel between two measurements, \bar{X} is the mean of the total voxels, and m is the number of the voxels. In addition, the CVs for the T_2 values of metabolites in the phantoms were calculated using the SD divided by the mean.

The 3D J-resolved MRSI data were referenced to the 3D SPGR image by assuming that there was no movement between the image and spectra acquisition. The FLAIR image was aligned to the corresponding 3D SPGR image. Segmentation of the 3D SPGR brain images were performed automatically using a hidden Markov random field model with an expectation-maximization algorithm (15). The segmented white matter mask was then used to identify voxels that had at least 85% normal appearing white matter or 85% gray matter. The tumor lesions were restricted to the voxels within the T_2 hyperintensities defined by T_2 -weighted images. To avoid errors in identification of normal voxels, the edges of the PRESS box and ventricles were excluded from the analysis. Voxels that satisfied the above criteria were used for comparative analyses in the volunteer and patient data. Nonparametric Wilcoxon rank sum tests were used to assess the differences for the metabolic relaxation times, with a P -value of 0.05 considered to be significant.

RESULTS

The oscillating coupling patterns for ²CH and ⁴CH₂ protons of Glu and Gln appear as pseudotriplets in the simulation, which makes it possible to leave only the center signal after averaging spectra with different echo times. The TE-averaged spectra of GAMMA simulations and single voxel phantom studies for pure Glu and Gln are shown in Fig. 1. The ⁴CH₂ Glu resonance is clearly resolved from the ⁴CH₂ Gln resonance both in simulations and in phantom studies with a chemical shift difference of 0.1 ppm.

Figure 2 shows the 2D J-resolved spectra recorded from the Lac phantoms with two localizations, one in the center

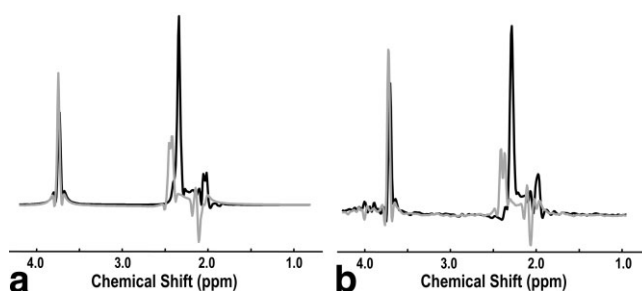


FIG. 1. Simulated (a) and phantom (b) TE-averaged PRESS spectra of Glu (black) and Gln (gray). The ⁴CH₂ Glu resonance is clearly resolved from the ⁴CH₂ Gln resonance in both simulations and phantom studies with a chemical shift difference of 0.1 ppm.

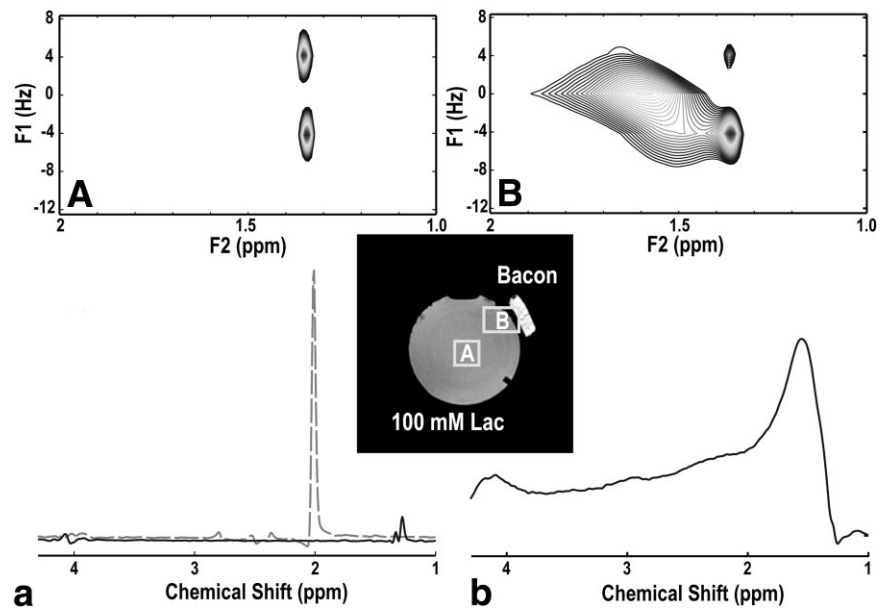
of the Lac phantom (voxel A) and the other contaminated with a part of bacon (voxel B). The J cross-peaks caused by the methyl group of Lac in the 2D spectrum were separated from the overlapping Lip peaks, which were compared with the 1D spectra extracted from $J = 0.0$ Hz (TE-averaged spectrum). For comparison with resonances without J couplings, the TE-averaged spectrum of the NAA phantom was coplotted with the Lac spectrum. As expected, the doublet resonances of Lac were cancelled in the TE-averaged spectra, but successfully displayed in the 2D spectrum.

The estimates of reproducibility were obtained using a voxel-by-voxel comparison of the peak heights of different metabolites. The values of CVs were 4% for Cho, 5% for Cr, 6% for NAA, and 9% for Glu in the phantom, compared with 15%, 16%, 12%, and 35% in vivo, respectively. The CVs were relatively higher in vivo, especially for Glu.

Figure 3 illustrates the result of 3D J-resolved MRSI data acquired from the phantom. The TE-averaged spectra offered an unobstructed single Glu peak and a doublet of mI. The cross-peaks of Lac in the 2D spectrum in the region between $F_2 = 1.5$ ppm and $F_2 = 1.0$ ppm were distinctly visualized within the three spatial dimensions despite the fact that there were only six echo times recorded. The T_2 values of Cho, Cr, and NAA in the phantom were 194 ± 14 ms, 296 ± 26 ms and 550 ± 72 ms (mean \pm SD). With CVs of 7% for Cho, 9% for Cr, and 13% for NAA, the T_2 values of metabolites were markedly uniform in the spectral array and could be used to reflect the regional T_2 difference in vivo.

In vivo TE-averaged MRSI data were obtained with good SNR over the entire spectral array. The SNR values of Cho, Cr, NAA, and Glu in volunteers were 17.0 ± 4.9 , 15.8 ± 4.5 , 33.4 ± 11.5 , and 4.3 ± 2.0 , respectively. An example of white matter and gray matter voxels from the volunteer acquired with 3D J-resolved MRSI is given in Fig. 4. Compared with each individual echo spectra, the TE-averaged spectra had flat baselines but maintained the metabolites that had relatively shorter T_2 values and thus provided more accurate quantification. The Glu/Cr levels were obviously higher in the gray matter voxel than those in white matter from the metabolic maps shown in Fig. 4. The ratios of mean metabolite levels in gray matter relative to white matter from six volunteers without corrections of relax-

FIG. 2. Single-voxel 2D J-resolved spectra from a 100 mM Lac phantom with two localizations (voxel A and voxel B). The 2D spectrum and the corresponding 1D spectrum were plotted. The TE-averaged spectra from 50 mM NAA phantom (dotted line) were coplotted with the Lac spectra. Voxel A was acquired with the voxel size of 8 cm³, a NEX of 4, and a TR of 10 s (total acquisition time ~4 min), and Voxel B was acquired with voxel size of 20 cm³, a NEX of 2, and a TR of 1.2 s (total acquisition time ~2 min).



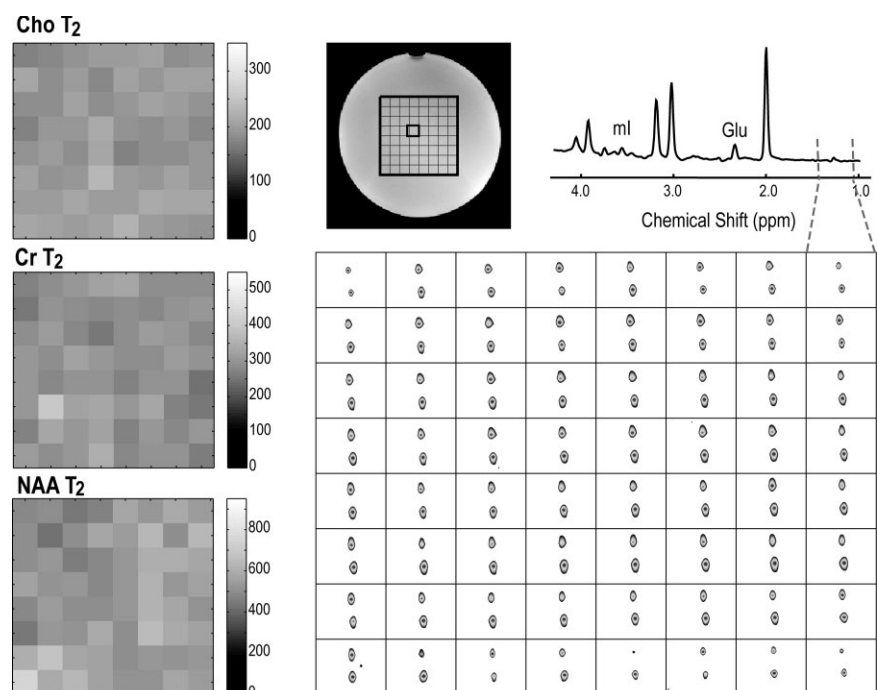
ation times were 1.0 ± 0.2 for Cho, 1.2 ± 0.1 for Cr, 0.9 ± 0.1 for NAA, 1.3 ± 0.2 for Glu, and 1.2 ± 0.2 for mI.

Figure 5 shows the TE-averaged spectra corresponding to the regions shown on the T_2 -weighted MRI image from a glioma patient. The spectra demonstrated good quality, and metabolic ratio maps represented the changes in the corresponding spectra well. The resonances of the Lac methyl group from the tumor could not be observed in the TE-averaged spectra but appeared as cross-peaks in the 2D spectrum. The relative metabolite ratios in patients quantified by LCModel without corrections of relaxation time compared with those in volunteers are shown in Table 1. As expected, the levels of Cho/Cr and mI/Cr increased in

the tumor lesions compared to the levels in the normal tissues, and NAA/Cr decreased.

From the volunteers, the T_2 values of Cho were shown to be statistically significantly higher in gray matter ($P = 0.004$) relative to white matter, while those of NAA were significantly higher in the white matter ($P < 0.001$). Compared with Cho and NAA, the T_2 values of Cr showed less tissue differences. Table 2 shows the T_2 values of Cho, Cr, and NAA in the segmented white matter and gray matter from the volunteers and the T_2 hyperintensity lesions from patients. Consistent with previous studies (7), the T_2 relaxation times of normal brain metabolites were different from the T_2 values in gliomas. The T_2 values of Cho and Cr

FIG. 3. 3D J-resolved MRSI acquired from the head phantom. The cross-peaks of Lac in the 2D spectra with the region between $F_2 = 1.5$ ppm and $F_2 = 1.0$ ppm were displayed in the 3D spatial dimensions, which was compared with the $J = 0$ Hz spectra extracted from the 2D spectra (TE-averaged spectra). The T_2 values of Cho, Cr, and NAA in the phantom were distributed uniformly in the spatial dimension.



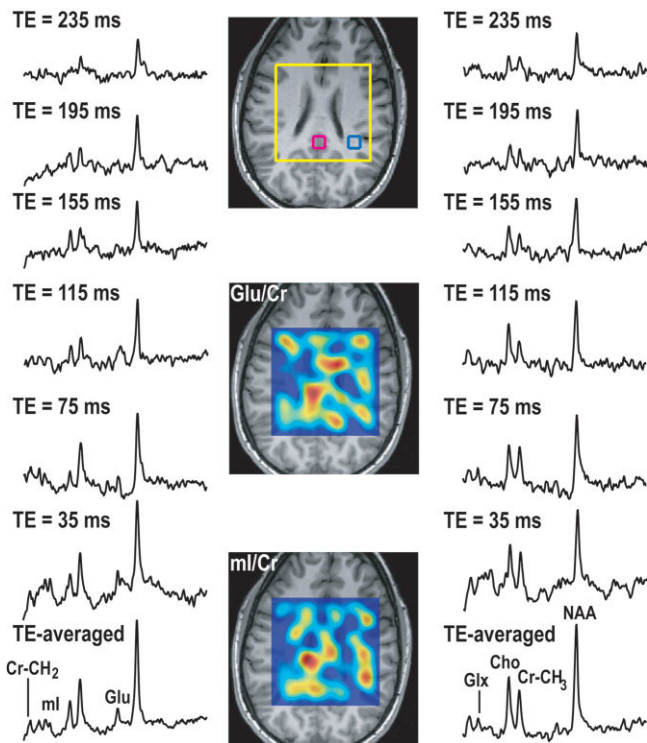


FIG. 4. 3D J-resolved MRSI acquired from a volunteer. The TE-averaged spectra from two voxels, gray matter and white matter, were plotted along each individual echo spectra. The metabolic maps were quantified using LCModel without corrections of relaxation time and plotted with the range between 0 and 2.20 for Glu/Cr and between 0 and 1.90 for ml/Cr.

in the lesions were statistically significantly longer than those in normal white matter ($P < 0.005$), while T_2 values of NAA were shorter, although without statistical significance.

DISCUSSION

A J-resolved MRSI sequence with localization in three spatial dimensions was implemented within a clinically feasible scan time at 3T (23 min). Postprocessing methods were applied for interpretation and quantification of metabolites from these spectra for normal volunteer and patients with brain tumor. This technique allows simultaneous quantification of Glu independent of Gln, visualization and quantification of Lac methyl protons in 2D spectra, as well as evaluation of changes of metabolite T_2 relaxation time, on a voxel-by-voxel (1-cm^3 resolution) basis in a large 3D volume, typically $\sim 256\text{ cm}^3$.

J-resolved spectroscopy is one of the simplest 2D sequences, which allows separation of metabolites based on both chemical shift and J-modulation. A major drawback of this acquisition is its relatively long acquisition time due to numerous t_1 increments required for wide bandwidth in the F_1 dimension to avoid aliasing and fine spectral resolution for the separation of J-coupling resonances. Previously developed measurements based upon TE-averaged PRESS, offered effective separation of the Glu signal from NAA and Gln at 3T by canceling the side bands of

triplets or quintuplets (6), as well as suppressing the doublet, such as from the methyl group of Lac. To implement this technique in three spatial dimensions within a feasible total scan time, relatively few points in t_1 are required. The t_1 values used in this study were modified both to optimize for detection of Glu in the TE-averaged spectra and to visualize Lac in the 2D spectrum, in addition to using the fewest number of t_1 points that allowed coverage in three spatial dimensions. Even spacing of 40 ms of echo time offers the possibility to visualize the Lac in the 2D spectrum, while more echo time points can provide more accurate T_2 fitting. If only the TE-averaged spectra are of interest, the last echo time spectra can be omitted. The bandwidth in the F_1 domain was small (~ 25 Hz) but large enough for the separation of methyl groups of Lac that have a spectral resolution of ~ 4.17 Hz.

The incorporation of the flyback echo-planar gradient readout scheme (9) was necessary to acquire the J-resolved MRSI data in human studies because it speeds up the data acquisition (23 min). The slight disadvantage of this method is the 12% to 22% loss in SNR per unit time for the flyback MRSI as compared with the conventional MRSI (9). In this case, the fast acquisition was critical to acquire the patient data and the SNR obtained from the in vivo data was adequate for quantification of the metabolites

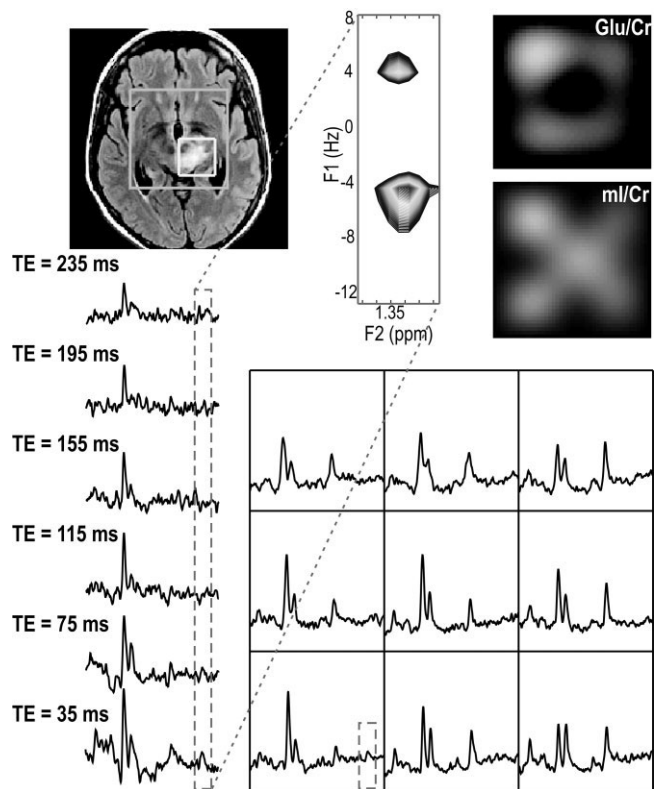


FIG. 5. 3D J-resolved MRSI acquired from a patient with glioma. The TE-averaged spectra corresponds to the location in the T_2 -weighted image. The 2D spectrum with the expanded region centered at 1.35 ppm extracted from the labeled voxel, which was compared with six individual echo time spectra. The metabolic maps of Glu/Cr and ml/Cr are plotted with the same scale as in Fig. 4.

Table 1

Relative Metabolite Levels Quantified by LCMoDel Without Corrections for Relaxation Time From Six Normal Volunteers and Four Patients With Primary Brain Tumors*

	Cho/Cr	NAA/Cr	Glu/Cr	Glx/Cr	mI/Cr
WM	0.34 ± 0.08	2.17 ± 0.50	1.77 ± 0.68	2.33 ± 1.29	1.48 ± 0.53
GM	0.26 ± 0.06	1.62 ± 0.45	1.91 ± 0.75	2.69 ± 1.34	1.38 ± 0.46
Patient A	0.57 ± 0.16	1.14 ± 0.33	1.47 ± 0.57	2.12 ± 1.36	1.61 ± 0.66
Patient B-D	0.40 ± 0.10	1.21 ± 0.39	1.63 ± 0.68	2.97 ± 3.01	1.57 ± 0.60
Total T_2 lesions	0.45 ± 0.14	1.20 ± 0.38	1.58 ± 0.64	2.74 ± 2.67	1.58 ± 0.62

*Numbers refer to mean ± SD.

WM = white matter, GM = gray matter.

targeted in our study. Since 16 spatial encodings are achieved in the flyback readout at 1-cm spatial resolution (16 cm FOV), aliasing from subcutaneous Lip into the region of interest can be eliminated along this direction (RL). One of the potential limitations of this technique is the need to trade off spectral bandwidth with spatial resolution and sampling efficiency. With the gradient system available on our clinical system, at spatial resolution of 1 cm³, the spectral bandwidth for the waveform designed for this study was 988 Hz, which was large enough to cover the metabolites of interest in the brain. Although the total acquisition time was shortened, there still could be some motion artifacts. The multiple echoes were chosen to be the inner loop while the phase-encoding steps were chosen to be the outer loop to minimize errors between echo times, but some spatial distortions may still exist and would be reflected as a smearing in the spatial domain.

Compared to short-echo MRSI data, the TE-averaged spectra have less contamination from macromolecules and offer unobstructed Glu, which allows more accurate quantification. The simplification of spectra is at the cost of generating a large dataset, which complicates the post-processing and may be time-consuming or require parallel processing. In this study, only the TE-averaged spectra ($F_1 = 0$ Hz) were quantified using LCMoDel (13) instead of using 2D fitting, such as ProFit (16), which may further improve quantitative accuracy. The methyl group of Lac was visualized in the 2D spectra and could also be quantified from the spectra extracted from the 2D spectra at $J = \pm 4.17$ Hz.

Estimates of reproducibility for Cho, Cr, and NAA demonstrated excellent results in phantoms: 4% for Cho, 5% for Cr, 6% for NAA, and 9% for Glu. These CV values were calculated based on a voxel-by-voxel basis using the peak

heights of metabolites. The estimates for Cho, Cr, and NAA in vivo were 15%, 16%, and 12%, respectively, slightly higher than those in the phantoms. Registration of the position of the PRESS localization volume between two scans (17) may help to improve these results. Although the TE-averaged spectra offered a single peak for Glu and less macromolecular contamination, it was possible that Glu was overestimated because of the inclusion of the short echo data in the TE-averaged spectra. The relatively large CV for Glu suggests that baseline fitting is still necessary for quantifying the TE-averaged spectra.

Ratios of relative metabolite levels without corrections of relaxation time were estimated in the regions of normal gray matter and white matter from volunteers and T_2 hyperintense lesions from gliomas. As expected, the ratio of Glu/Cr was slightly higher in the gray matter, while mI/Cr was higher in the white matter due to the Cr being higher in gray matter. The ratios of mean metabolites for Glu and mI were higher in the gray matter, which is consistent with a previous study (8). Data from three GBM patients showed that Glx/Cr was increased in the T_2 hyperintense lesions and Glu/Cr was reduced, which suggests an increase of Gln in these patients. These in vivo studies demonstrated good quality and are extremely promising.

The T_2 relaxation times of Cho, Cr, and NAA were also estimated from these 3D data. The small variances obtained from the phantom suggested that the procedure used to estimate T_2 values was reliable. The mean T_2 values of metabolites were similar to prior studies (18), and the differences in T_2 values between normal white matter and T_2 hyperintensity lesions were consistent with previous work (7). This may offer a new index for characterizing tumors.

In conclusion, phantoms and in vivo experiments showed that the 2D J-resolved approach was successful in detecting unobstructed metabolite peaks corresponding to Cho, Cr, NAA, mI, Glu, and Lac from the simplified spectra along with the flat baseline, and simultaneously allowed estimation of T_2 values of the singlets. The SNR of the 2D J-resolved 3D MRSI performed on the human clinical 3T scanner was able to provide excellent spatial and spectral resolution within the human brain. After establishing procedures for the acquisition, reconstruction, and quantification of 2D J-resolved PRESS MRSI with three spatial dimensions, this methodology can be incorporated into protocols being used to evaluate patients with glioma and may provide improved characterization of the tumors.

Table 2

T_2 Relaxation Times of Metabolites From Six Volunteers and Four Primary Brain Tumor Patients*

	Cho	Cr	NAA
WM	205 ± 77 (192) <i>N</i> = 217	148 ± 35 (145) <i>N</i> = 219	314 ± 105 (299) <i>N</i> = 298
GM	265 ± 81 (248) <i>N</i> = 12	155 ± 41 (142) <i>N</i> = 27	221 ± 66 (216) <i>N</i> = 39
Total T_2 lesions	245 ± 94 (222) <i>N</i> = 83	174 ± 50 (166) <i>N</i> = 46	322 ± 160 (260) <i>N</i> = 59

*Numbers refer to mean ± SD (median) in ms, and *N* represents the number of voxels involved in the group.

WM = white matter, GM = gray matter.

ACKNOWLEDGMENTS

We thank Dr. Ying Lu, Professor of Radiology and Biostatistics, University of California, San Francisco (UCSF), for his expert assistance in the statistical aspects for this project. We also thank Esin Ozturk-Isik, Eugene Ozhinsky, Duan Xu, Mark Albers, and Janine Lupo for useful discussions and assistance.

REFERENCES

1. Star-Lack J, Spielman D, Adalsteinsson E, Kurhanewicz J, Terris DJ, Vigneron DB. In vivo lactate editing with simultaneous detection of choline, creatine, NAA, and lipid singlets at 1.5 T using PRESS excitation with applications to the study of brain and head and neck tumors. *J Magn Reson* 1998;133:243–254.
2. Kelley DA, Wald LL, Star-Lack JM. Lactate detection at 3T: compensating J coupling effects with BASING. *J Magn Reson Imaging* 1999;9:732–737.
3. Thomas MA, Ryner LN, Mehta MP, Turski PA, Sorenson JA. Localized 2D J-resolved 1H MR spectroscopy of human brain tumors in vivo. *J Magn Reson Imaging* 1996;6:453–459.
4. Jensen JE, Frederick BD, Wang L, Brown J, Renshaw PF. Two-dimensional, J-resolved spectroscopic imaging of GABA at 4 Tesla in the human brain. *Magn Reson Med* 2005;54:783–788.
5. Govindaraju V, Young K, Maudsley AA. Proton NMR chemical shifts and coupling constants for brain metabolites. *NMR Biomed* 2000;13:129–153.
6. Hurd R, Sailasuta N, Srinivasan R, Vigneron DB, Pelletier D, Nelson SJ. Measurement of brain glutamate using TE-averaged PRESS at 3T. *Magn Reson Med* 2004;51:435–440.
7. Li Y, Srinivasan R, Chang S, Nelson SJ. Characterization of high grade gliomas using TE-averaged PRESS at 3 T. In: Proceedings of the 14th Annual Meeting of ISMRM, Seattle, WA, USA, 2006 (Abstract 1778).
8. Srinivasan R, Cunningham C, Chen A, Vigneron D, Hurd R, Nelson S, Pelletier D. TE-averaged two-dimensional proton spectroscopic imaging of glutamate at 3 T. *Neuroimage* 2006;30:1171–1178.
9. Cunningham CH, Vigneron DB, Chen AP, Xu D, Nelson SJ, Hurd RE, Kelley DA, Pauly JM. Design of flyback echo-planar readout gradients for magnetic resonance spectroscopic imaging. *Magn Reson Med* 2005;54:1286–1289.
10. Smith SA, Levante TO, Meier BH, Ernst RR. Computer simulations in magnetic resonance: an object-oriented programming approach. *J Magn Reson* 1994;106:75–105.
11. Crane JC, Crawford FW, Nelson SJ. Grid enabled magnetic resonance scanners for near real-time medical imaging processing. *J Parallel Distrib Comput* 2006;66:1524–1533.
12. Li Y, Osorio JA, Ozturk-Isik E, Chen AP, Xu D, Crane JC, Cha S, Chang S, Berger MS, Vigneron DB, Nelson SJ. Considerations in applying 3D PRESS H-1 brain MRSI with an eight-channel phased-array coil at 3 T. *Magn Reson Imaging* 2006;24:1295–1302.
13. Provencher SW. Estimation of metabolite concentrations from localized in vivo proton NMR spectra. *Magn Reson Med* 1993;30:672–679.
14. Nelson SJ. Analysis of volume MRI and MR spectroscopic imaging data for the evaluation of patients with brain tumors. *Magn Reson Med* 2001;46:228–239.
15. Zhang Y, Brady M, Smith S. Segmentation of brain MR images through a hidden Markov random field model and the expectation-maximization algorithm. *IEEE Trans Med Imaging* 2001;20:45–57.
16. Schulte RF, Boesiger P. ProFit: two-dimensional prior-knowledge fitting of J-resolved spectra. *NMR Biomed* 2006;19:255–263.
17. Hancu I, Blezek DJ, Dumoulin MC. Automatic repositioning of single voxels in longitudinal 1H MRS studies. *NMR Biomed* 2005;18:352–361.
18. Traber F, Block W, Lamerichs R, Gieseke J, Schild HH. 1H metabolite relaxation times at 3.0 Tesla: measurements of T1 and T2 values in normal brain and determination of regional differences in transverse relaxation. *J Magn Reson Imaging* 2004;19:537–545.